Carbohydrate Research 344 (2009) 1085–1094

Contents lists available at ScienceDirect

Carbohydrate Research

journal homepage: www.elsevier.com/locate/carres

Structural reorganization of molecular sheets derived from cellulose II by molecular dynamics simulations

Hitomi Miyamoto [a], Myco Umemura [b], Takeshi Aoyagi [c], Chihiro Yamane [a,*], Kazuyoshi Ueda [d], Kazuhiro Takahashi [a]

[a] Faculty of Home Economics, Kobe Women's University, 2-1 Aoyama, Higashisuma Suma-ku, Kobe 654-8585, Japan
[b] Graduate School of Biostudies, Kyoto University, Oiwake-cho, Kitashirakawa, Sakyo-ku, Kyoto 606-8502, Japan
[c] Central R&D Laboratories, Asahi Kasei Corporation, 2-1 Samejima, Fuji, Shizuoka 416-8501, Japan
[d] Graduate School of Engineering, Yokohama National University, 79-5 Tokiwadai, Hodogaya-ku, Yokohama 240-8501, Japan

ARTICLE INFO

Article history:
Received 11 November 2008
Received in revised form 12 March 2009
Accepted 17 March 2009
Available online 20 March 2009

Keywords:
Molecular dynamics (MD) simulation
Initial structure
Regenerated cellulose
Structural formation mechanism
Molecular sheet

ABSTRACT

We investigated structural reorganization of two different kinds of molecular sheets derived from the cellulose II crystal using molecular dynamics (MD) simulations, in order to identify the initial structure of the cellulose crystal in the course of its regeneration process from solution. After a one-nanosecond simulation, the molecular sheet formed by van der Waals forces along the $(1\bar{1}0)$ crystal plane did not change its structure in an aqueous environment, while the other one formed by hydrogen bonds along the (1 1 0) crystal plane changed into a van der Waals-associated molecular sheet, such as the former. The two structures that were calculated showed substantial similarities such as the high occupancy of intramolecular hydrogen bonds between $O3^{H}$ and O5 of over 0.75, few intermolecular hydrogen bonds, and the high occurrence of hydrogen bonding with water. The convergence of the two structures into one denotes that the van der Waals-associated molecular sheet can be the initial structure of the cellulose crystal formed in solution. The main chain conformations were almost the same as those in the cellulose II crystal except for a $-16°$ shift of φ (dihedral angle of O5–C1–O1–C4) and the *gauche–gauche* conformation of the hydroxymethyl side group appears probably due to its hydrogen bonding with water. These results suggest that the van der Waals-associated molecular sheet becomes stable in an aqueous environment with its hydrophobic inside and hydrophilic periphery. Contrary to this, a benzene environment preferred a hydrogen-bonded molecular sheet, which is expected to be the initial structure formed in benzene.

1. Introduction

Regenerated cellulose is one of the most hydrophilic polymers. Contact angles of water droplets on cellophane and cuprophane, which are typical regenerated cellulose films, are 11.6° and 12.2°, respectively, which are far lower than those of widely used polymers such as poly(vinyl alcohol) (PVA), 36°; starch, 41°; poly(methyl methacrylate), 57°; poly(vinyl acetate), 63°; nylon, 70°; poly(vinylidene chloride), 80°; poly(vinyl chloride), 87°; poly(styrene), 91°; poly(ethylene), 94°; poly(propylene), 95°; and poly(tetrafluoroethylene), 108°.[1,2] It is worthy to note that the contact angle of regenerated cellulose is lower than that of water-soluble polymers such as PVA and starch. The high wettability of regenerated cellulose is considered to be derived from the uniplanar orientation of the $(1\bar{1}0)$ crystal plane that is parallel to the film surface. Many hydroxyl groups are geometrically present on the surface of the $(1\bar{1}0)$ plane, whereas hydrogen atoms exist on the (1 1 0) crystal plane; therefore, it is reasonable to conclude that many hydroxyl groups on the film surface results from the uniplanar orientation of the $(1\bar{1}0)$ plane, and this imparts high hydrophilicity to regenerated cellulose.

Although regenerated cellulose is applied in many fields including textiles and medical use, the high wettability of it prevents its application fields from expanding, due to its low wrinkle properties and shrinkage in washing for textile use, and activation of the immune system in medical use. For instance, when regenerated cellulose is used for artificial kidneys, the complement in blood is activated due to the influence of hydroxyl groups of cellulose, and the number of leucocytes decreases, resulting in undesirable effects on patients. In this situation, it is necessary to understand how regenerated cellulose is formed from solution and how the structures of regenerated cellulose can be controlled in order to create new application fields for regenerated cellulose. A probable mechanism for the structural formation of regenerated cellulose from cellulose solutions has been proposed as follows:[1,3]

* Corresponding author. Tel.: +81 (0)78 737 2348; fax: +81 (0)78 732 5161.
E-mail address: yamane@suma.kobe-wu.ac.jp (C. Yamane).

0008-6215/$ - see front matter © 2009 Elsevier Ltd. All rights reserved.
doi:10.1016/j.carres.2009.03.014

(i) Glucopyranose rings are stacked together by hydrophobic interaction with van der Waals forces, and molecular sheets are formed.
(ii) Association of these sheets by hydrogen bonds affords thin planar crystals incorporating amorphous chains.
(iii) These structures, which are randomly dispersed in solution, contact and adhere with each other to form three-dimensional structures.

The first step of this mechanism (i) is difficult to verify by experimental procedures because there is almost no way to understand the molecular structures, such as conformation, dynamics, and molecular details. The purpose of this study, thus, is to identify the initial structure from cellulose solutions by computer simulation methods.

Computer simulation has been used for many studies of cellulosic materials. Research using miniature crystal models of cellulose, which was one of the most representative simulation studies, revealed that cellulose II has the lowest calculated energy for cellulose polymorphism, followed by Iα, III_I, ramie I, IV_{II}, and IV_I.[4] Only the topmost surface layer of crystalline cellulose was structurally affected by water outside the surface, which was consistent with the findings based on solid state ^{13}C CP-MAS NMR spectroscopy.[5–7] Models of crystal allomorphs (Iβ and Iα) were consistent with experimental data such as density, energy difference, conformational aspects, and hydrogen bonding networks, and an amorphous structure was proposed in view of conformational behavior.[8] Significant changes occur in crystal structures surrounded by water. These include expansion of the unit cell, change in the γ angle to almost orthogonal, a right-hand twist of approximately 1.5° per cellobiose unit, and a 14.8° tilt of the sugar rings in the center chains, resulting in a transition from the *trans-gauche* (*tg*) to *gauche–gauche* (*gg*) conformation, forming interlayer hydrogen bonds to the origin chains.[9] Crystal models of cellulose Iβ and Iα are twisted and form a slightly right-handed shape in aqueous environments, although other structural features are almost equal to those of the original crystal, despite such an overall deformation.[10,11] Thus, there has been a wide range of computational studies on cellulose, but there has been almost no attempt to elucidate the structural formation and the starting structure of cellulose crystal from solution except the report by Cousins and Brown.[12] These researchers have reported that the cellulose molecular sheets packed by hydrophobic interaction could be the starting structure to form cellulose I crystals because its potential energy is lower than that of hydrogen-bonded molecular sheets, using molecular mechanics (MM) calculation.

In this paper, we investigated the initial structures derived from cellulose solutions using molecular dynamics (MD) simulation to confirm the mechanism for the structural formation of regenerated cellulose. We prepared two kinds of molecular sheet models based on the cellulose II crystal as initial structure. One was sliced off along the (1 1 0) crystal plane of cellulose II formed by intermolecular hydrogen bonds, and the other exposed its $(1\bar{1}0)$ crystal plane that is hydrophobically packed. Structural changes in the conformations of main chain and side groups, tilt angles of glucopyranose rings with sheet planes, and hydrogen bonding systems of these two molecular sheets in water and benzene solvent were investigated using MD simulation in order to identify the initial structure of the cellulose crystal from these environments.

2. Computational procedures

Two kinds of molecular sheets were sliced off along the (1 1 0) and $(1\bar{1}0)$ crystal planes from the cellulose II crystal model[13] containing four cellotetraoses in each (Fig. 1). The former and the latter were referred as a hydrogen-bonded (HB) (A in Fig. 1) and a van der Waals-associated (VW) (B in Fig. 1) mini-sheet because they were formed by intermolecular hydrogen bonds of $O2^H\cdots O2$, $O6^H\cdots O6$, $O6^H\cdots O5$, and $O6^H\cdots O3$, and van der Waals forces, respectively. Here, atomic nomenclature and partial charges are shown in Figure 2 and Table 1, respectively. The mini-sheet was placed in the bottom of a periodic box with 240 water or 50 benzene molecules in it at a density of 1.00 g/cm^3 or 0.87 g/cm^3, respectively. The periodic box with four cellotetraoses (16 glucose residues) and 240 water or 50 benzene molecules was adjacent to the next boxes with full periodic boundary conditions, where the glucose residues were covalently bonded across the periodic boxes in the chain direction, in order to give the model infinite chain length.

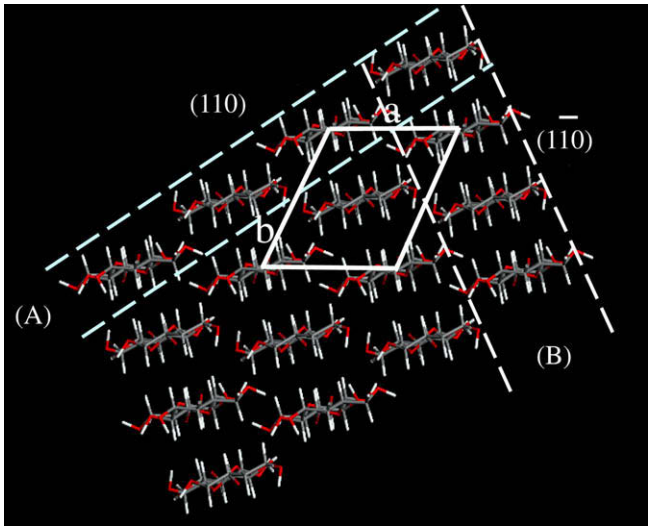

Figure 1. Cellulose II crystal and the models of molecular sheets: (A) hydrogen-bonded (HB) molecular sheet; (B) van der Waals-associated (VW) molecular sheet.

The system was first heated to 498 K in order to anneal the water or benzene molecules, while the cellulose chains were fixed at their initial position during 30 ps with 1.0 fs time step in an *NVT* ensemble using the NOSE thermostat. After the annealing, we removed the positional restraints of the cellulose chains and calculated each system at 298 K under 1000 hPa for 1 ns with 1.0 fs time step in an *NPT* ensemble using full periodic boundary conditions. The Ewald method was used for the calculation of Coulombic interaction with a 9.5 Å cut-off length of nonbonding energy. We chose the COMPASS force field (ACCELRYS Software Inc.), and NOSE

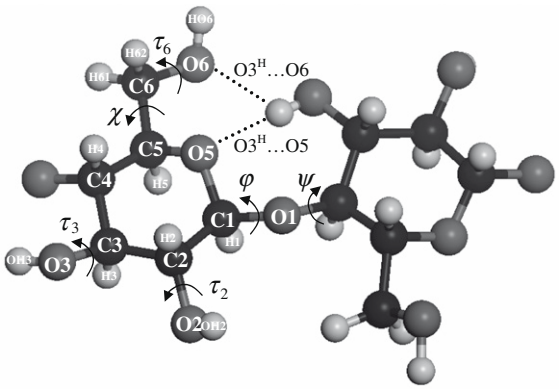

Figure 2. Atomic labeling and torsion-angle parameters: φ = O5–C1–O1–C4, ψ = C1–O1–C4–C3, χ = C4–C5–C6–O6, τ_2 = C1–C2–O2–H2, τ_3 = C2–C3–O3–H3, and τ_6 = C5–C6–O6–H6.

Table 1
Partial atomic charges

Atom	Charges
Cellulose	
C1	0.2670
C2,3,4,5	0.1070
C6	0.0540
O1,5	−0.3200
O2,3,6	−0.5700
H1,2,3,4,5,61,62	0.0530
HO2,3,6	0.4100
Water	
O	−0.8200
OH1,2	0.4100
Benzene	
C1,2,3,4,5,6	−0.1268
CH1,2,3,4,5,6	0.1268

thermostat and the Parrinello–Raman barostat for the calculation that could well converge the system energy without divergence.

We calculated the cellulose II crystal itself in the *NPT* ensemble without water and benzene molecules in order to verify the COMPASS force field for 1 ns simulation with the same conditions as the other systems. The unit cell dimensions after the calculation were $a = 8.08$ Å, $b = 8.92$ Å, $c = 10.35$ Å, and $\gamma = 116.1°$, which were quite similar to the original dimensions of the cellulose II crystal ($a = 8.01$ Å, $b = 9.04$ Å, $c = 10.36$ Å, and $\gamma = 117.1°$)[13] in which the deviation was only −0.87%, −1.33%, +0.10%, and −0.85%, respectively. The dihedral angles after the calculation were φ (O5–C1–O1–C4) = −101° and ψ (C1–O1–O4–C3) = 95°, which were also similar to the reported ones[14–16] such as −91.3 to −97.6° for φ and 87.0–95.8° for ψ. The hydroxymethyl dihedral angles remained unchanged, in the *gauche–trans* (*gt*) conformation after the calculation. From these results, it seems reasonable to conclude that the COMPASS force field is adequate for this study.

3. Results and discussion

3.1. Water environment

3.1.1. Changes of molecular sheets in water environment

The hydrogen-bonded (HB) mini-sheet corresponding to the (1 1 0) crystal plane in the cellulose II crystal could not maintain the original structure in a water medium (Fig. 3). The glucopyranose rings stood up and contacted with each other at the ring plane after the 1 ns calculation. Consequently, the HB mini-sheet changed into a van der Waals-associated (VW) mini-sheet, which had almost no intermolecular hydrogen bonds. The camber angles made by the plane of glucopyranose rings and the interface between the mini-sheet and water increased from 18° (at 0 ns, Fig. 3a) to 90° (at 1 ns, Fig. 3b, hVW hereafter). The equatorial direction of the glucopyranose ring is hydrophilic because all three hydroxyl groups are protruded in this direction. In contrast, the axial direction of the ring is hydrophobic because the hydrogen atoms of C–H bonds are located axially. Therefore, the above result is reasonable because the hVW structure, having a hydrophilic periphery and a hydrophobic interior, must be much more stable in water medium than the HB structure. The dimensions of the periodic box were changed by the simulation as follows: before simulation in Figure 3a, $a = 20.6$ Å (depth, cellulose chain direction), $b = 29.2$ Å (width, cellulose molecular sheet direction), $c = 22.4$ Å (height), $\alpha = \beta = \gamma = 90.0°$; after simulation in Figure 3b, $a = 20.8$ Å, $b = 21.3$ Å, $c = 30.7$ Å, $\alpha = 61.9°$, $\beta = 103.6°$, $\gamma = 122.1°$. The lengths and angles of the periodic cell can be independently changed in keeping its parallelepiped shape by the Parrinello–Rahman barostat. The rearrangement of the molecular sheet, changing from a hydrogen-bonded mini-sheet to a van der Waals-associated mini-sheet, shortened the width of the molecular sheet because intermolecular distance in the hydrogen-bonded mini-sheet is larger than that of the van der Waals-associated mini-sheet. This corresponded to the shortening of the *b* axis of the cell. If the *b* axis cannot be shortened, the molecular sheet must be divided into two or more pieces in the periodic boundary cells. The length of the *a* axis remained unchanged, which corresponded to the length of four glucose residues. Therefore, the *c* axis must be elongated in order to maintain constant pressure, temperature and particle numbers. For these reasons, we selected the Parrinello–Rahman barostat. It should be noted that the volume of the starting cell (Fig. 3a) was slightly larger than that of the rearranged cell (Fig. 3b) because of the rather lower density of the starting cell at the initial stage of the calculation at which the cellulose layer and water layer were combined.

Although a large number of studies have been made on models of microcrystalline cellulose such that the structural changes at the top surface differ on each crystal plane in a water environment as reported by Heiner et al.,[6] little is known about MD simulations that make use of a model of cellulose molecular sheets for the purpose of elucidating structural formation from cellulose solutions.

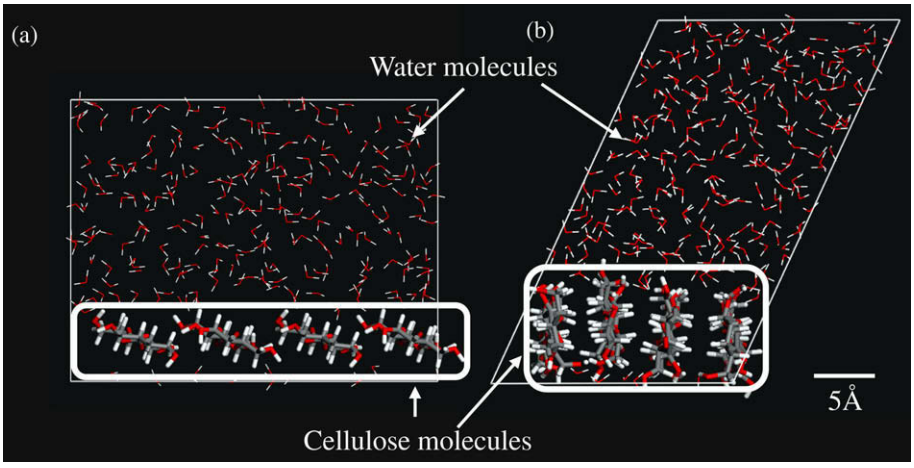

Figure 3. Changes in hydrogen-bonded (HB) mini-sheets in water media: (a) before calculation; (b) after 1 ns calculation (hVW structure). The original sheet (a) is sliced off along the (1 1 0) plane of cellulose II, and has four cellotetraoses, that is, 16 glucose residues. The periodic box has 240 water molecules.

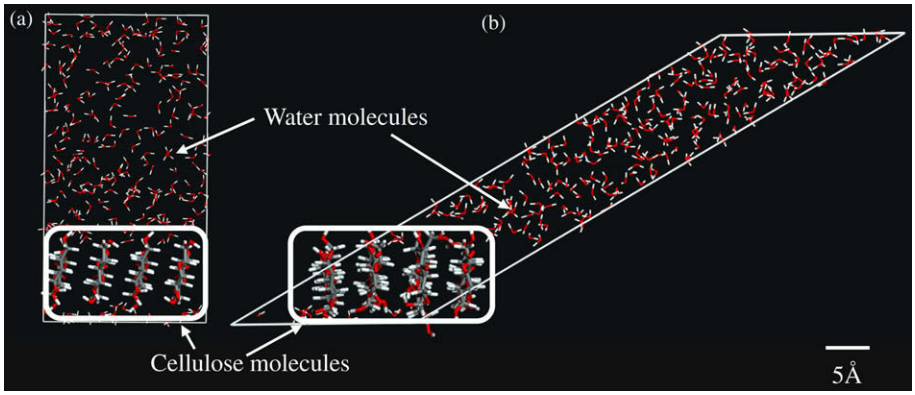

Figure 4. Changes in van der Waals-associated (VW) mini-sheets in water media: (a) before calculation; (b) after 1 ns calculation (vVW structure). The original sheet (a) is sliced off along the $(1\bar{1}0)$ plane of cellulose II and has four cellotetraoses, that is, 16 glucose residues. The periodic box has 240 water molecules.

In contrast to the HB mini-sheet, the VW mini-sheet along the $(1\bar{1}0)$ plane has a hydrophobic interior and a hydrophilic periphery that remained unchanged in the water medium after 1 ns simulation (Fig. 4). The camber angle was slightly changed from 102° to 91° during the MD calculation, which possibly allows the hydroxyl groups of the glucopyranose rings to access the water molecules more easily. We refer to the final structure from VW as vVW (Fig. 4b) hereafter. In both final structures, hVW and vVW, the hydrophobic interior and hydrophilic periphery, allowed them to be stable in water. The periodic box parameters changed from before simulation in Figure 4a; $a = 20.6$ Å, $b = 17.9$ Å, $c = 33.9$ Å, $\alpha = \beta = \gamma = 90.0°$ to after-simulation values shown in Figure 4b; $a = 20.8$ Å, $b = 17.7$ Å, $c = 63.4$ Å, $\alpha = 39.4°$, $\beta = 120.9°$, $\gamma = 93.4°$.

3.1.2. Hydrogen bonding

Table 2 shows the degree of intra- and intermolecular hydrogen bonds in the hVW and vVW structures. Only hydrogen bonds with a maximum occupancy ratio above 0.05 are reported. The criteria used for identification of hydrogen bonds were that the A–H distance should be less than 2.8 Å and the D–H–A angle should be greater than 110°, where A and D designate acceptor and donor atoms, respectively. Occupancy is the ratio of a number of hydrogen bonds to that of the possible A and D pairs; the measurement covers all glucose residues. The major intramolecular hydrogen bond in cellulose II is $O3^{H}\cdots O5$ in addition to the minor one of $O3^{H}\cdots O6$ (Fig. 2).[14] The atoms with superscript letter H indicate the donor atoms of the hydrogen bonds. The occupancy ratio of the intra-chain hydrogen bond of $O3^{H}\cdots O5$ was 0.75 and 0.78 in the hVW and vVW structure, whereas that of $O3^{H}\cdots O6$ was only 0.26 and 0.39, respectively. This might correspond to the major and minor components in the original hydrogen bonds, and/or might be due to greater hydrogen bonding with water at the O6 position than at the O5 position (Table 3). There was almost no hydrogen bonding between water and the O5 position. The low occupancy ratio of $O6^{H}\cdots O2$ intra-chain hydrogen bond formation in the vVW structure was well correlated with the appearance of the small peak of the *tg* conformation shown in Figure 5a, by which the $O6^{H}\cdots O2$ intra-chain hydrogen bond could be formed.

Table 2
Intramolecular and intermolecular hydrogen bonds in molecular sheets in water[a]

	Intramolecular hydrogen bonds			Intermolecular hydrogen bonds
	$O3^{H}\cdots O5$	$O3^{H}\cdots O6$	$O6^{H}\cdots O2$	$O6^{H}\cdots O2$
hVW[b] mini-sheet	0.75	0.26	< 0.05	0.08
vVW[b] mini-sheet	0.78	0.39	0.08	0.13

[a] The number listed is the occupancy, that is, the probability of existence of the hydrogen bond. Only hydrogen bonds with a maximum occupancy above 0.05 are reported. The donor is given first.
[b] hVW and vVW mini-sheet mean the molecular structures reorganized from hydrogen-bonded and van der Waals-associated mini-sheet in water, respectively.

Table 3
Hydrogen bonds between cellulose and water[a]

	hVW[b] mini-sheet			vVW[b] mini-sheet		
	Donor	Accepter	Total	Donor	Accepter	Total
O2	1.02	1.06	2.08	1.04	0.88	1.92
O3	0.52	0.77	1.29	0.65	0.90	1.55
O4	—	0.00	0.00	—	0.00	0.00
O5	—	0.00	0.00	—	0.03	0.03
O6	0.98	0.98	1.96	0.67	1.17	1.84

[a] The number listed is the occupancy, that is, the probability of existence of the hydrogen bond.
[b] hVW and vVW mini-sheet mean the molecular structures reorganized from hydrogen-bonded and van der Waals-associated mini-sheet in water, respectively.

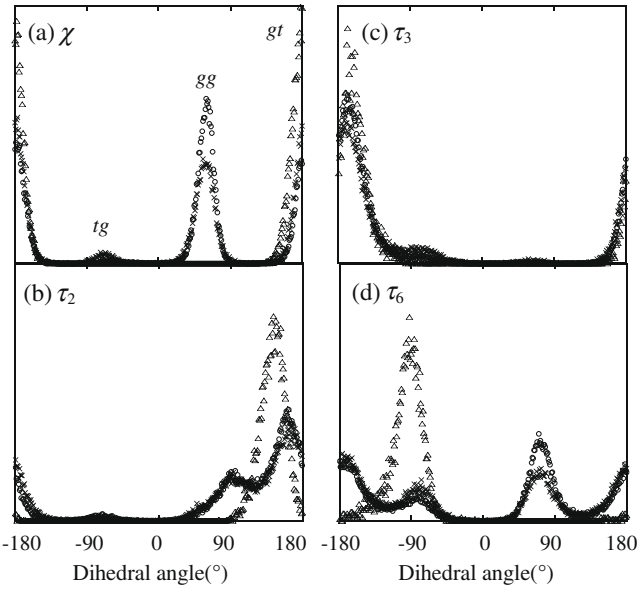

Figure 5. Torsion angle distribution of side groups in water: (a), χ (C4–C5–C6–O6); (b), τ_2 (C1–C2–O2–H2); (c), τ_3 (C2–C3–O3–H3); (d), τ_6 (C5–C6–O6–H6). ○, hVW structure; ×, vVW structure; Δ, reorganized crystal model. Each torsion angle is averaged against all glucose residues for the last 200 ps in a 1 ns simulation.

Intermolecular, that is, inter-chain hydrogen bonds in the original HB mini-sheet along the (1 1 0) crystal plane are $O2^{H}\cdots O2$ and $O6^{H}\cdots O6$ as major components, and $O6^{H}\cdots O5$ and $O6^{H}\cdots O3$ as minor components before the calculation. All these inter-chain hydrogen bonds completely disappeared after the 1 ns simulation, indicating that the HB mini-sheet changed into a VW-like mini-sheet (hVW structure) in the water medium. A new inter-chain hydrogen bond, $O6^{H}\cdots O2$, appeared instead with a low occupancy ratio of 0.08, which cannot be formed in the cellulose II crystal because the O6 and O2 atoms are located so far from each other as not to form a hydrogen bond. The occurrence of the inter-chain hydrogen bond of $O6^{H}\cdots O2$ in vVW structure, 0.13, which was not found in the original VW structure, is probably due to the *c*/4 shift of adjacent chains along the chain direction. According to the study by Tanaka and Fukui,[17] hydrogen bonds between hydroxyl groups of cellulose chains were not detected in the aqueous environment due to interruption by water molecules around the cellulose chains. This result well corresponds to our study, including the extremely low degree of intermolecular hydrogen-bond formation. The two final structures of vVW and hVW from two opposite mini-sheets resemble each other quite well, except for the slightly higher degree of intra- and inter-chain hydrogen bonding in the former than the latter.

The degree of hydrogen bonding with water was the highest for O2, followed by O6 and O3, except for O2 as an acceptor in the vVW structure (Table 3). This order corresponds to the degree of intramolecular and intermolecular hydrogen bonding in the mini-sheets. The O3 atom contributed to the intra-chain hydrogen bonds of $O3^{H}\cdots O5$ and $O3^{H}\cdots O6$ as a donor atom. The exceptional low value of the O2 atom as an acceptor in the vVW (0.88) corresponds to the formation of intra- and intermolecular hydrogen bonds $O6^{H}\cdots O2$. The sum of the occupancy of three kinds of hydrogen bond (with water, intra-, and inter-molecule) exceeds 2 for each atom (O2, O3, and O6), meaning that there are more than two hydrogen bonds for each atom. It is reasonable to conclude that the highly developed hydrogen bond system allows both the vVW and hVW structures to be stable in water. On the other hand, there are almost no hydrogen bonds with water at O4 and O5 probably due to their interior positions in the sheets.

3.1.3. Conformation of side groups and the main chain

Figures 5a–d show the torsion angle distributions of the hydroxymethyl side group (χ (C4–C5–C6–O6)) and hydroxyl groups at C2, C3, and C6 (τ_2 (C1–C2–O2–H2), τ_3 (C2–C3–O3–H3), and τ_6 (C5–C6–O6–H6)). As a result, these side group conformations were almost the same between the vVW and hVW structure after the 1 ns simulation, and agreed well with the hydrogen bonding system especially for χ.

The χ value showed three low-energy conformations (*gg*, *gt*, *tg*) whose ratio of *gg*:*gt*:*tg* are 0.41:0.54:0.05, and 0.54:0.44:0.02 in the vVW and hVW structures, respectively. Only the *gt* conformation was found in the reorganized cellulose crystal. The torsion angle distribution of χ agrees well with the manner of hydrogen bonding. The appearance of the *gg* conformation is probably due to the hydrogen bonds with water, because the hydroxyl group at C6 protrudes into water so as to assume the *gg* conformation, which is the lowest energy one for β-D-glucopyranose.[18–21] The higher ratio of *gt* in vVW (occupancy, 0.54) than that in hVW (0.44) corresponds well to the higher order intramolecular hydrogen bond of $O3^{H}\cdots O6$ in vVW (0.39) than in hVW (0.26), because the *gt* conformation is required for the intramolecular $O3^{H}\cdots O6$ hydrogen bond. In addition, the low percentage of the *tg* conformation in both the vVW (0.05) and hVW (0.02) structure that is necessary for the $O6^{H}\cdots O2$ intramolecular hydrogen bond also correlates with the low occupancy of the $O6^{H}\cdots O2$ intramolecular hydrogen bond in the vVW (0.08) and hVW (<0.05) structure, respectively (Table 2).

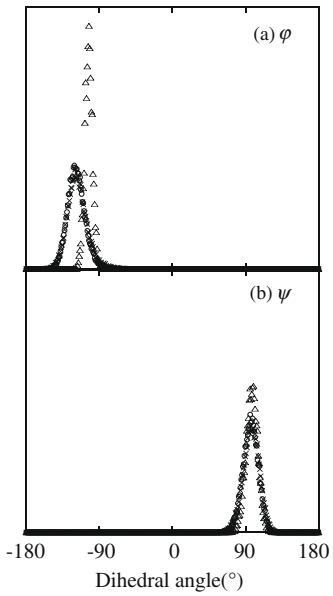

Figure 6. Torsion angle distribution of main chains in water: (a) φ(O5–C1–O1–C4); (b) ψ (C1–O1–C4–C3). ○, hVW structure; ×, vVW structure; Δ, reorganized crystal model. Each torsion angle is averaged against all glucose residues for the last 200 ps in a 1 ns simulation.

The τ_2 angle distribution showed two rather broad peaks after simulations for both vVW and hVW, whereas only one peak was observed for the reorganized crystal (Fig. 5b). This bifurcation is probably due to the hydrogen bonds of the O2 atom with water (Table 3). The distribution of the τ_3 dihedral angle in the vVW and hVW structures was quite similar to that in the reorganized crystal (Fig. 5c), corresponding to the well-developed intramolecular hydrogen bonds of $O3^{H}\cdots O5$ and $O3^{H}\cdots O6$ (Table 2). Three peaks could be observed for the τ_6 dihedral (Fig. 5d) in both mini-sheets, despite there being only one peak for the reorganized crystal. The reason for the triplet has not been made clear, but the diversity of hydrogen bonds in the mini-sheets must be responsible for these widely varying distributions. Even in a crystal (modeled structure of cellulose Iβ), Mazeau reported that τ_2 and τ_6 adopted a wide range of values, whereas τ_3 was comparable to that observed in crystallography.[22]

The distribution of dihedral angles φ (O5–C1–O1–C4) and ψ (C1–O1–C4–C3) can depict the cellulose backbone conformation (Fig. 6). The peak top angles of φ of both mini-sheets (−117°) and that of the reorganized crystal (−101°) were slightly different (Fig. 6a). This deviation in φ by −16° between both mini-sheets and the reorganized crystal indicates that the molecules in the mini-sheets have a right-handed twist conformation.[9,11] The distributions of φ of vVW and hVW were almost the same. The distributions of ψ were also similar among vVW, hVW, and the reorganized crystal (Fig. 6b), where the peak angles were in the range of 90–95°, values that correspond to the other experimental results.[14–16]

3.1.4. Mechanism for the structural formation of regenerated cellulose in water

The two simulated mini-sheets, starting from hydrogen-bonded mini-sheet (HB) along the (1 1 0) crystal plane, and the van der Waals forces associated mini-sheet (VW) along the (1 $\bar{1}$ 0) crystal plane, had similar structures including the side-group and main-chain conformations, the hydrogen-bonding system, and the camber angle. These two simulated structures were formed by van der Waals forces with few intermolecular hydrogen bonds and many

hydroxyl groups linked with many water molecules at the periphery. In other words, the simulated structures possessed a hydrophobic interior and a hydrophilic periphery, allowing them to be stable in water. Therefore, we conclude that the structural formation of regenerated cellulose from an aqueous cellulose solution can start from a structure like the simulated mini-sheets. Incorporating these results into known experimental results,[23] we propose the mechanism for the structural formation of regenerated cellulose from polar solution as follows in (i)–(iii).

(i) When an aqueous cellulose solution experiences unstable conditions, for example, the addition of a precipitate or undergoing a substantial temperature increase, the cellulose molecules seem to aggregate side by side, with glucopyranose rings stacking by hydrophobic interactions to form a sheet structure as schematically shown in Figure 7a. The existence of this sheet structure, necessary for this hypothesis of structural formation, has been suggested by many studies: for example, a certain kind of dye in bacterial cellulose production systems prevented crystallization to form molecular sheets with a thickness of only 1–2 glucan chains.[24–26] Hayashi[27] and Hermans[28] identified such layer structures (calling them plane lattice structures or sheet-like structures) as a basic feature of regenerated cellulose. An energetics study using the MM3 molecular mechanics program indicated that the potential energy of molecular sheets formed by van der Waals forces was far lower than that of hydrogen-bonded molecular sheets in water.[12] It is reasonable to assume that a two-dimensional structure exists in the process of structural formation between the one-dimensional (molecule) and three-dimensional structures (crystal and amorphous), and the molecular sheet structure formed by van der Waals forces is the one most likely to result as a two-dimensional structure.

(ii) As the precipitation proceeds, many sheet structures are progressively stacked by hydrogen bonds to form thin planar crystals that incorporate amorphous regions. Some aggregates that are tightly stacked with each other without any defects become crystalline regions. In contrast, others piled up with some defects become amorphous regions (Fig. 7b). From this mechanism, the amorphous regions in regenerated cellulose can be defined as being composed of molecular sheets with distances that have substantial distributions; Hayashi[27] and Hermans[28] also made similar definitions regarding the amorphous state.

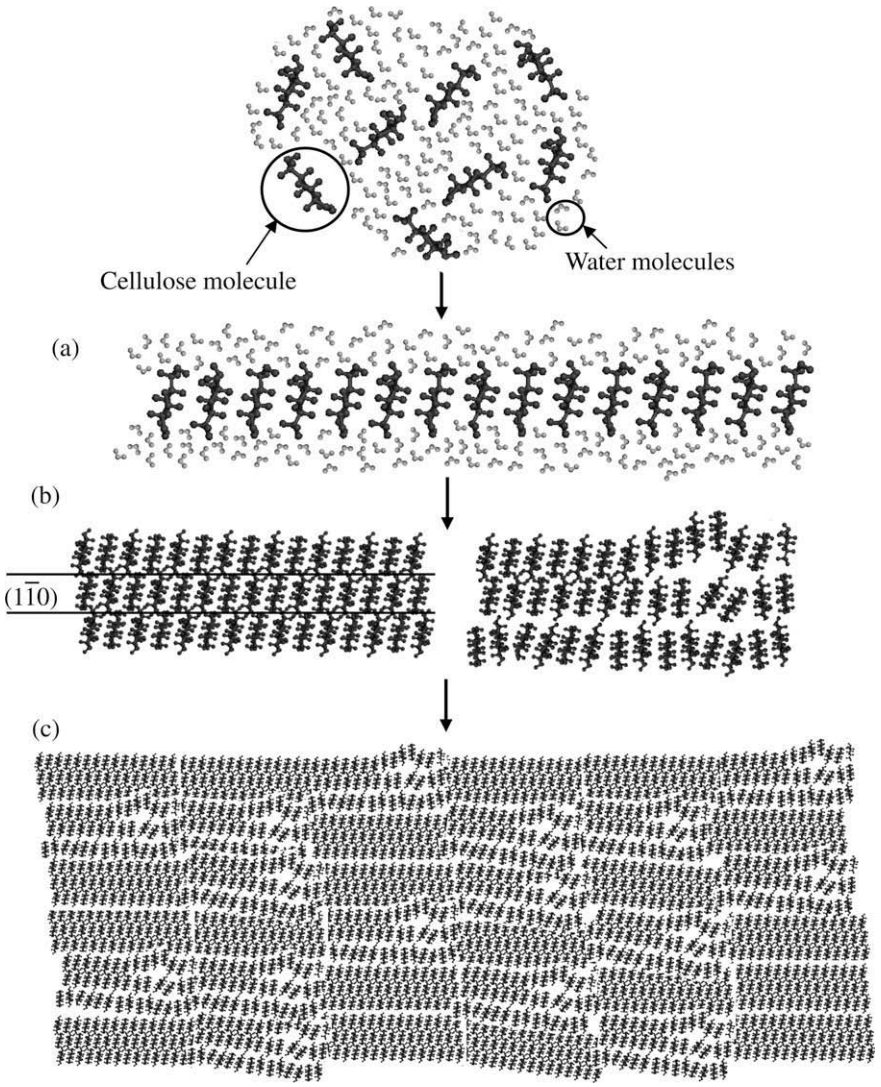

Figure 7. Schematic model for the structural formation of regenerated cellulose in a water environment: (a) formation of the molecular sheets by van der Waals force; (b) piling up of the molecular sheets by hydrogen bonds to form seeds of crystal and amorphous; (c) contact and sticking together of the structural unites to form regenerated cellulose.

(iii) At this stage, these randomly dispersed structural units contact and adhere together by a diffusion-limited cluster–cluster aggregation mechanism[3,29] to form a mixture of crystalline and amorphous regions (Fig. 7c) and are shaped into regenerated cellulose. At the same time, the solvent is squeezed out from the precipitating cellulose gel material, resulting in shrinkage, which causes a uniplanar orientation of the $(1\bar{1}0)$ crystal plane and leads to the wettable surface of the regenerated cellulose materials.[1]

There are many dissolving systems such as water,[30,31] sodium hydroxide,[1,32] *N*-methyl morpholine *N*-oxide (NMMO),[33] Viscose, and Cupra. The structural formation, that is the stacking of glucopyranose rings to form molecular sheets leading to crystallization, might be prevented by interactions between solvents and the hydroxyl groups of cellulose. Specifically, the crystallinity (Xc) of regenerated cellulose from these dissolving systems decreases in the following order: water, Xc = 78.3%[31] > simple interaction of solvent; NaOH, Xc = 45.5%[32] > complexes; NMMO, Xc = 38–41%[33] and Cupra, Xc = 38.2–43.4%[32] > derivatives; Viscose, Xc = 21.5–29.2%.[32] This order probably corresponds to the degree of steric hindrance and degree of decomposition of derivatives and complexes during the precipitation process of these systems. Despite these impediments to structure formation, the uniplanar orientation of the $(1\bar{1}0)$ plane is still maintained in every system, and the films from the real systems have quite low contact angles. For example, the uniplanar orientation indexes $f(1\bar{1}0)$ are 0.67 for the NaOH, 0.60 for the Cupro, and 0.57 for Viscose systems. Contact angles of the water droplets are 10.5° for NaOH, 12.2° for Cupro, and 11.6° for Viscose.[1] It should be noted that the orientation index $f(1\bar{1}0)$ provides a relative degree of planar orientation and takes on values from 0 (random) to 1 (complete parallel to surface). Therefore, it is possible that the mechanism for structural formation of regenerated cellulose proposed here using the ideal system can be applied to the real systems using polar solvent systems such as NaOH, NMMO, Cupra, and Viscose.

3.2. Benzene environment

A benzene environment provides results that differ from those of a water environment. Fig. 8 shows the apparent changes in the molecular mini-sheets in a benzene environment. Basically, the HB mini-sheet retained its shape, but changed slightly to a wavy structure after 1 ns in the MD simulation (Fig. 8a). In other words, the intermolecular hydrogen bonds appeared to play the role of hinge-like joints. Hereafter, this mini-sheet was referred to as hHB structure. In spite of the wavy structure, the inter- and intramolecular hydrogen bonds were highly developed, and the main-chain conformation scarcely changed from its original position, as will be described later. The periodic box parameters were changed from $a = 20.6$ Å, $b = 29.2$ Å, $c = 25.4$ Å, $\alpha = \beta = \gamma = 90.0°$ to $a = 20.7$Å, $b = 31.5$Å, $c = 57.3$Å, $\alpha = 29.4°$, $\beta = 132.3°$, $\gamma = 109.6°$ (hHB structure, Fig. 8a).

The VW mini-sheet fell into a disordered state (Fig. 8b), but began to form a few intermolecular hydrogen bonds. This mini-sheet was referred to as vHB structure, that is, it is a hydrogen-bonded mini-sheet that changed from a van der Waals-associated mini-sheet in a benzene medium. This vHB structure seems to be in a transitional state toward a molecular sheet with highly developed intermolecular hydrogen bonds, such as the hHB structure. The periodic box parameters were changed from $a = 20.6$ Å, $b = 17.9$ Å, $c = 36.1$ Å, $\alpha = \beta = \gamma = 90.0°$ to $a = 20.9$ Å, $b = 21.0$ Å, $c = 48.9$ Å, $\alpha = 135.4°$, $\beta = 133.4°$, $\gamma = 73.8°$ (vHB structure, Fig. 8b).

Table 4 shows the occupancy ratio of intra- and intermolecular hydrogen bonds after MD simulation. In general, the degree of this hydrogen bonding in the benzene environment was higher than that in the water environment, probably due to lack of competitive hydrogen bonds with water. Especially in the hHB structure, almost all the atoms capable of forming intramolecular hydrogen bonds were occupied with hydrogen bonds; 0.98 for $O3^{H}\cdots O5$ and 0.90 for O2···O6 including $O6^{H}\cdots O2$ and $O2^{H}\cdots O6$, whereas there were no O2···O6 intramolecular hydrogen bonds in the original cellulose II crystal. In spite of the disordered appearance of the

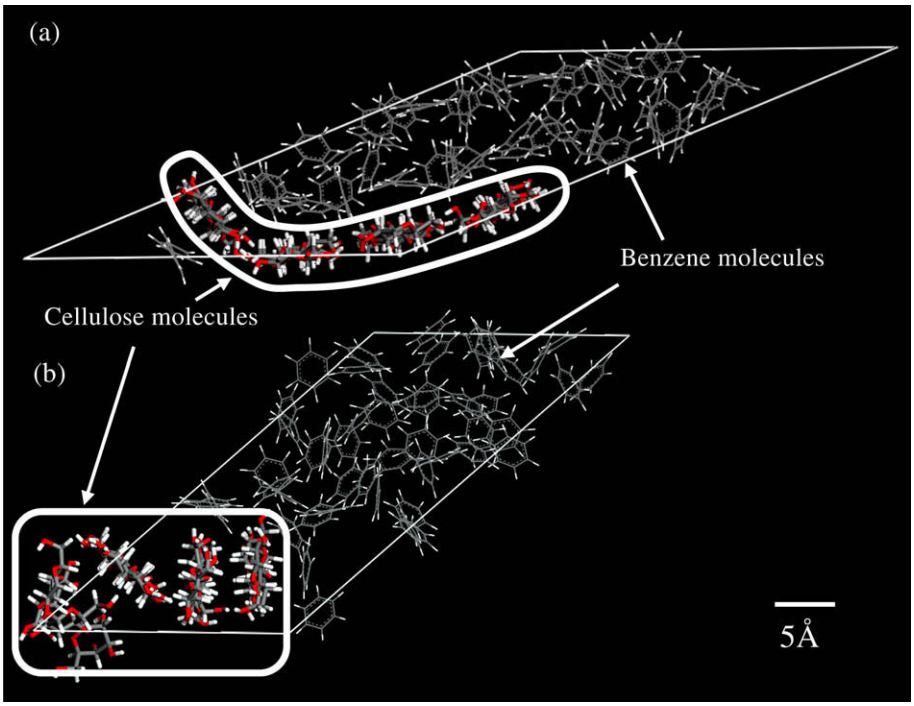

Figure 8. Changes in cellulose mini-sheets in benzene media after 1 ns calculation: (a) hHB structure reorganized from the hydrogen-bonded crystal plane; (b) vHB structure reorganized from the van der Waals-associated crystal plane. The original sheets are sliced off along the (1 1 0) and $(1\bar{1}0)$ plane of cellulose II for (a) and (b), respectively, and have four cellotetraoses, that is, 16 glucose residues. The periodic box has 50 benzene molecules.

Table 4
Intramolecular and intermolecular hydrogen bonds in molecular sheets in benzene[a]

	Intramolecular hydrogen bonds				Intermolecular hydrogen bonds			
	$O3^H\cdots O5$	$O3^H\cdots O6$	$O6^H\cdots O2$	$O2^H\cdots O6$	$O6^H\cdots O2$	$O2^H\cdots O6$	$O6^H\cdots O3$	$O2^H\cdots O2$
hHB[b] mini-sheet	0.98	0.12	0.52	0.38	0.26	0.43	0.28	0.10
vHB[b] mini-sheet	0.75	0.35	0.23	0.08	0.06	0.05	0.13	<0.05

[a] The number listed is the occupancy, that is, the probability of existence of the hydrogen bond. Only hydrogen bonds with a maximum occupancy above 0.05 are reported. The donor is given first.
[b] hHB and vHB mini-sheet mean the molecular structures reorganized from hydrogen-bonded and van der Waals-associated mini-sheet in benzene, respectively.

vHB structure, the degree of intramolecular hydrogen bonding of $O3^H\cdots O5$ was rather high, at 0.75. However, it was not surprising to have such high occupancy, because the degree of $O3^H\cdots O5$ intramolecular hydrogen bonding in cello-oligosaccharides, from dimers to hexamers, has been calculated to be over 0.6 at every degree of polymerization, from 2 to 6, even in water.[34] The report also concluded that cello-oligosaccharides were less flexible in aqueous solution, because of the well-formed intramolecular hydrogen bonds of $O3^H\cdots O5$.

Intermolecular hydrogen bonds originally existing in the HB mini-sheet along the (1 1 0) crystal plane are $O6^H\cdots O6$ and $O2^H\cdots O2$ as major components, and $O6^H\cdots O5$ and $O6^H\cdots O3$ as minor components. In the hHB structure, the intermolecular hydrogen bonding system was rearranged after 1 ns simulation: $O6^H\cdots O6$ vanished and $O2^H\cdots O2$ remained at only 0.10; $O6^H\cdots O5$ disappeared and $O6^H\cdots O3$ was still present at 0.28; O2···O6 was rearranged to form a higher occupancy ratio of 0.69, adding together donors and acceptors. The rearrangement may result from the approximate $c/4$ shift of the center or origin chains in the chain direction so that the two glucopyranose rings of the center and origin chains may be adjacent to each other. The level of intermolecular hydrogen bonds in the vHB structure was rather low, but higher than that of the mini-sheets in a water medium (vVW and hVW structures).

The ratios of occupancy in χ for the hHB and vHB structures and the reorganized crystal were *gg*:*gt*:*tg* = 0.36:0.07:0.57, 0.43:0.46:0.11, and 0:1.00:0, respectively, as shown in Figure 9. The marked decrease in *gt* and the substantial increase in *tg* for the hHB structure corresponded well with the cleavage of the intramolecular hydrogen bond of $O3^H\cdots O6$ (occupancy, 0.12) and the newly formed intramolecular hydrogen bond of O2···O6 (occupancy including donor and acceptor, 0.90). The vHB structure displayed the same trend, but it was not noticeable, that is, the occupancy of $O3^H\cdots O6$ was 0.35 and that of O2···O6 was 0.31. The appearance of the *gg* rotamer was probably due to its low-energy conformation in an isolated glucose residue.[18] The distributions of τ_2 and τ_3 in the mini-sheets mainly consisted of two peaks and one peak, respectively. The two roles of the O2 atom, as donor and acceptor, to form intramolecular hydrogen bonds of $O2^H\cdots O6$ and $O6^H\cdots O2$ could be responsible for the two peaks of τ_2. Similarly, the highly developed intramolecular hydrogen bonding of $O3^H\cdots O5$, where the O3 atom acted as donor, could account for the one τ_3 peak. Three broad peaks were observed for the τ_6 dihedral. Various kinds of intra- and intermolecular hydrogen bonds could account for these widely varying distributions. The main-chain conformations, φ and ψ, after simulations are shown in Figure 10, and were quite similar to those in a water environment (Fig. 6), indicating that the backbone conformations were independent of the surroundings. The peak top angles of φ for vHB, hHB, and reorganized crystal were −117°, −114°, and −101°, respectively. The cellulose molecules in the both mini-sheets were expected to have a right-handed twist conformation. However, the slight shift of φ of hHB to higher angle from that of vHB (approximately 3°) was observed. The highest developed intra- and intermolecular hydrogen bonds in the hHB among these mini-sheets might restrain the molecules from right-handed twisting. The peak top angles of ψ for both mini-sheets and the reorganized crystal were 90–95° (Fig. 10b), which were of the same value as those obtained from the aqueous medium.

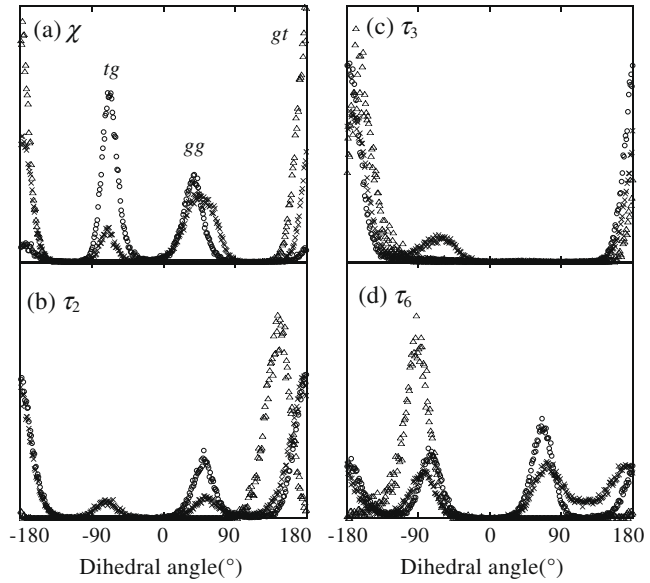

Figure 9. Torsion angle distribution of side groups in benzene: (a) χ (C4–C5–C6–O6); (b) τ_2 (C1–C2–O2–H2); (c) τ_3 (C2–C3–O3–H3); (d) τ_6 (C5–C6–O6–H6). ○, hHB structure; ×, vHB structure; Δ, reorganized crystal model. Each torsion angle is averaged against all glucose residues for the last 200 ps in a 1 ns simulation.

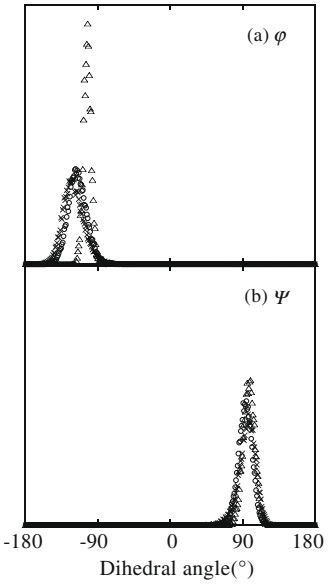

Figure 10. Torsion angle distribution of main chains in benzene: (a) φ(O5–C1–O1–C4); (b) ψ (C1–O1–C4–C3). ○, hHB structure; ×, vHB structure; Δ, reorganized crystal model. Each torsion angle is averaged against all glucose residues for the last 200 ps in a 1 ns simulation.

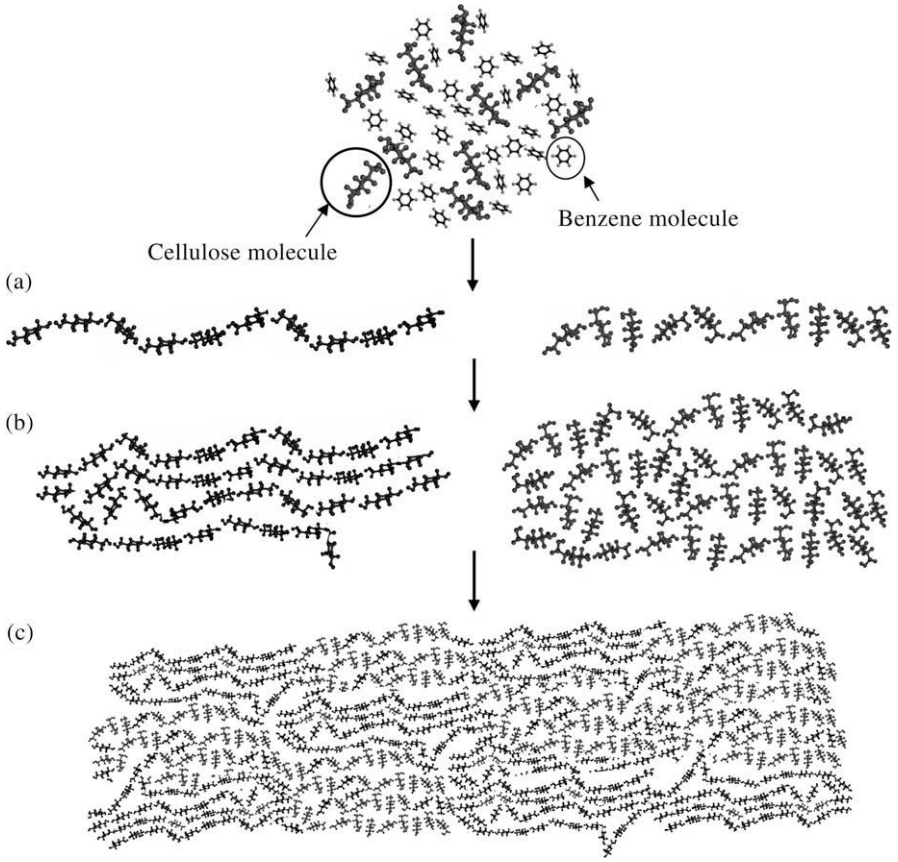

Figure 11. Schematic model for the structural formation of regenerated cellulose in a benzene environment.

Figure 11 shows the structural formation mechanism for regenerated cellulose in a benzene environment. Firstly, cellulose molecules associate to form sheet structures by intermolecular hydrogen bonding, where intermolecular hydrogen bonds appeared to be hinge-like joints, allowing them to have a wavy structure. Next, the molecular sheets stack together by hydrophobic interaction to form mainly amorphous regions, and these regions then contact each other to form larger structural units and to complete the regenerated cellulose structure. The regenerated cellulose precipitated by solvents with low dielectric constant, such as toluene, has a very low crystallinity index (Xc = 6%), whereas the Xc of the regenerated cellulose prepared from the aqueous system is high.[1] These experimental observations support the proposed mechanism.

4. Conclusions

The structural rearrangement of two different kinds of molecular sheets derived from cellulose II crystals was studied by MD simulation. The van der Waals-associated mini-sheet (VW), sliced off from the $(1\,\bar{1}\,0)$ crystal plane, remained apparently unchanged in the water medium. In contrast, the hydrogen-bonded mini-sheet (HB) along with the (1 1 0) crystal plane lost its intermolecular hydrogen bonds and changed into a van der Waals-associated mini-sheet (hVW structure). There were many structural similarities between these two mini-sheets rearranged in water: (1) the intramolecular hydrogen bonds of $O3^{H}\cdots O5$ were highly developed with occupancy values of over 0.75, whereas there were few intermolecular hydrogen bonds with those of about 0.1. (2) There were many hydrogen bonds with water so that the occupancy of hydrogen bonds, which are the sum of three kinds of hydrogen bonds for each atom (O2, O3, and O6), exceeded 2, which indicated that there were more than two hydrogen bonds for each atom. (3) The main-chain conformations were almost the same as those in the cellulose II crystal, except that the dihedral angles φ were shifted slightly to lower angle by $-16°$. (4) The *gg* conformation of the hydroxymethyl side group appeared, probably due to the formation of hydrogen bonds with water and the energetic stability of glucopyranose residues in water. In the course of rearrangements in water, two different kinds of molecular sheets converged into one, such as the van der Waals sheet structure, suggesting that the initial structure from the cellulose aqueous solution, where cellulose was dispersed molecularly, was that of the van der Waals-associated molecular sheets. It is not surprising that the van der Waals-associated molecular sheets are stable in aqueous media, because of their hydrophilic exterior and hydrophobic interior. However, in a benzene environment, the structure remaining after MD simulation was the hydrogen-bonded molecular sheet, which is expected to be the initial structure in benzene.

References

1. Yamane, C.; Aoyagi, T.; Ago, M.; Sato, K.; Okajima, K.; Takahashi, T. *Polym. J.* **2006**, *38*, 819–826.
2. Kitahara, F. Surface Properties. In *Kagakubinran II (Chemistry Handbook II)*, 3rd ed.; The Chemical Society of Japan: Tokyo, 1984. p 90.
3. Kiyose, M.; Yamamoto, E.; Yamane, C.; Midorikawa, T.; Takahashi, T. *Polym. J.* **2007**, *39*, 703–711.
4. French, D. A.; Miller, P. D.; Aabloo, A. *Int. J. Biol. Macromol.* **1993**, *15*, 30–36.
5. Heiner, P. A.; Teleman, O. *Langmuir* **1997**, *13*, 511–518.
6. Heiner, P. A.; Kuutti, L.; Teleman, O. *Carbohydr. Res.* **1998**, *306*, 205–220.
7. Newman, R. H.; Hemmingson, J. A. *Cellulose* **1994**, *2*, 95–110.
8. Mazeau, K.; Heux, L. *J. Phys. Chem. B* **2003**, *107*, 2394–2403.
9. Matthews, F. J.; Skopec, E. C.; Mason, E. P.; Zuccato, P.; Torget, W. R.; Sugiyama, J.; Himmel, E. M.; Brady, J. W. *Carbohydr. Res.* **2006**, *341*, 138–152.

10. Yui, T.; Nishimura, S.; Akiba, S.; Hayashi, S. *Carbohydr. Res.* **2006**, *341*, 2521–2530.
11. Yui, T.; Hayashi, S. *Biomacromolecules* **2007**, *8*, 817–824.
12. Cousins, K. S.; Brown, R. M., Jr. *Polymer* **1995**, *36*, 3885–3888.
13. Langan, P.; Nishiyama, Y.; Chanzy, H. *Biomacromolecules* **2001**, *2*, 410–416.
14. Langan, P.; Nishiyama, Y.; Chanzy, H. *J. Am. Chem. Soc.* **1999**, *121*, 9940–9946.
15. Stipanovic, A.; Sarko, A. *Macromolecules* **1976**, *9*, 851.
16. Kolpak, K. J.; Blackwell, J. *Macromolecules* **1976**, *9*, 273.
17. Tanaka, F.; Fukui, N. *Cellulose* **2004**, *11*, 33–38.
18. Kuttel, M.; Brady, J. W.; Naidoo, K. J. *J. Comput. Chem.* **2002**, *23*, 1236–1243.
19. Bock, K.; Duus, J. Ø. *J. Carbohydr. Chem.* **1994**, *13*, 513–543.
20. Nishida, Y.; Ohrui, H.; Meguro, H. *Tetrahedron Lett.* **1984**, *25*, 1575–1578.
21. Horii, F.; Hirai, A.; Kitamaru, R. In *The Structures of Cellulose: Characterization of the Solid States*; Atalla, R. H., Ed.; American Chemical Society: Washington, DC, 1987; pp 119–134.
22. Mazeau, K. *Cellulose* **2005**, *12*, 339–349.
23. Okajima, K.; Yamane, C. *SEN'IGAKKAISHI* **2001**, *57*, 156–162.
24. Malcolm Brown, R., Jr.; Haigler, C.; Cooper, K. *Science* **1982**, *218*, 1141–1142.
25. Kai, A.; Koseki, T. *Makromol. Chem.* **1985**, *186*, 2609–2614.
26. Halgler, H. C.; Chanzy, H. *J. Ultrastruct. Mol. Struct. Res.* **1988**, *98*, 299–311.
27. Hayashi, J.; Masuda, S.; Watanabe, S. *Nippon Kagaku Kaishi* **1974**, *5*, 948.
28. Hermans, H. P. *J. Polym. Sci.* **1949**, *4*, 145–151.
29. Kolb, M.; Botet, R.; Jullien, R. *Phys. Rev. Lett.* **1983**, *51*, 1123.
30. Deguchi, S.; Tsujii, K.; Horikoshi, K. *Green Chem.* **2008**, *10*, 191–196.
31. Sasaki, M.; Adshiri, T.; Arai, K. *AIChE J.* **2004**, *50*, 192–202.
32. Yamane, C.; Mori, M.; Saito, M.; Okajima, K. *Polym. J.* **1996**, *28*, 1039–1047.
33. Fink, H.-P.; Weigel, P.; Purz, H. J.; Bohn, A. *Recent Res. Dev. Polym. Sci.* **1998**, *2*, 387–403.
34. Umemura, M.; Yuguchi, Y.; Hirotsu, T. *J. Mol. Struct. THEOCHEM.* **2005**, *730*, 1–8.